

Continuous Emission of X-rays by Thermal Excitation of Six LiTaO₃ Single Crystals

This article has been downloaded from IOPscience. Please scroll down to see the full text article.

2011 IOP Conf. Ser.: Mater. Sci. Eng. 18 092034

(<http://iopscience.iop.org/1757-899X/18/9/092034>)

View [the table of contents for this issue](#), or go to the [journal homepage](#) for more

Download details:

IP Address: 24.118.174.49

The article was downloaded on 11/10/2011 at 14:21

Please note that [terms and conditions apply](#).

Continuous Emission of X-rays by Thermal Excitation of Six LiTaO₃ Single Crystals

Hiroyuki Honda¹, Shinji Fukao¹, Yang Guan¹, Yoshikazu Nakanishi¹,
Yuuki Sato¹, Yoshiaki Ito² and Shinzo Yoshikado¹

¹Graduate School of Engineering, Doshisha University, Kyotanabe,
Kyoto 610-0321, Japan

²Institute for Chemical Research, Kyoto University, Gokasyo, Uji,
Kyoto 611-0011, Japan

E-mail: syoshika@mail.doshisha.ac.jp

Abstract. The X-ray emission method using a pyroelectric crystal has intermittent emission and intensity is low. In order to achieve the continuous emission of X-rays, six LiTaO₃ single crystals are used. Furthermore, in order to investigate the emission of electrons by the interaction between the case material of an X-ray source and emitted X-rays, the case material with different work function or fluorescence yield, such as oxygen-free copper, stainless steel or aluminium, is used. It was found that the intensity of X-rays was depended on case material and it became high with decreasing the fluorescence yield of the case material. It was suggested that a part of emitted electrons were by the Auger process.

1. Introduction

Spontaneous polarization of a pyroelectric crystal such as LiNbO₃ or LiTaO₃ is dependent on the temperature of the crystal, and electric charge appears on the crystal surface by heating or cooling the crystal. Because of this pyroelectricity, intense electric fields appear around the crystal when the temperature changes. The electric fields accelerate electrons toward the crystal, a target faced to it and the case. As a result, X-rays are emitted by the impact of electrons against them [1, 2].

At the present time, X-ray tubes are generally used as an X-ray source. An X-ray tube requires an electron source, a high voltage power supply, and a cooling system. They restrict miniaturization and reduce X-ray emission efficiency. On the other hand, because the method of X-ray emission using pyroelectric crystals requires only a change of the crystal temperature, both the miniaturization and the improvement of the efficiency can be achieved. It is expected that a miniaturized X-ray source can be used as a compact diagnostic equipment or a compact analytical instrument. However, this method also has disadvantages such as intermittent emission or low intensity compared with an X-ray tube.

It was reported that compared with the case of using one pyroelectric crystal, the total intensity of X-rays in one period was more than twice when two crystals was placed oppositely and the temperature change of them was opposite in phase [2]. In Ref. 2, it was suggested that the intensity of X-rays increased with increasing auxiliary electrons emitted by the interaction between the case material of an X-ray source and emitted X-rays such as photoelectric effect. It is well known that the Auger effect easily occurs if the material has low fluorescence yield, namely, the small atomic number

[4]. It is therefore expected that more Auger electrons can be supplied if the material with the small atomic number such as aluminum is used.

Thus, in order to achieve continuous emission of X-rays with high intensity, six LiTaO₃ single crystals are used and the phase of the temperature change of each crystal is adjusted adequately. It is difficult to use seven or more crystals because of the viewpoints of a design of the X-ray source. Moreover, in order to investigate the detail of the interaction, the case material with different work function or fluorescence yield, such as oxygen-free copper, stainless steel or aluminium, is used.

2. Experiments

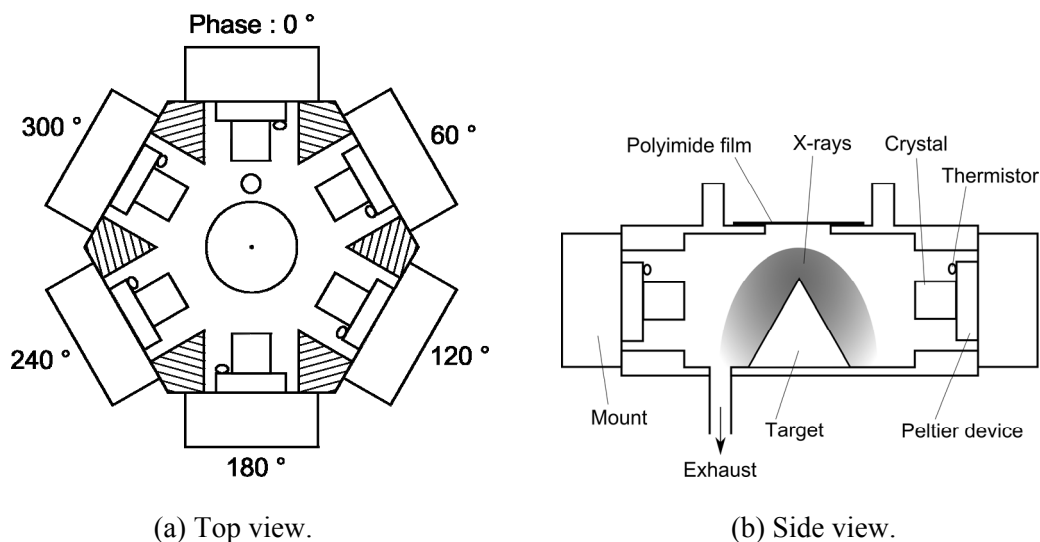
The photograph of the X-ray source fabricated for this study is shown in Figure 1. Six nonstoichiometric LiTaO₃ single crystals with the size of 5 mm × 5 mm × 5 mm were used. The electrical surfaces (z surface) which were perpendicular to the *c*-axis were mirror polished. The case material was oxygen-free copper (Cu), stainless steel (SUS304) or aluminum (Al). The target was cone-shaped niobium with 16 mm in height, 15 mm in width and an apex angle of 60°. It was placed in the center of the case as shown in Figure 2. The positively charged surface (+z surface) of each crystal was adhered to a Peltier device with silver paste. The six crystals were placed hexagonally around the target so that the negatively charged surface (−z surface) of each crystal could be faced to the target. The case, the target and the +z surface were electrically grounded.

The temperature of the crystals was changed by applying triangular wave voltages to the Peltier devices, and the temperature range ΔT was fixed at approximately 40 °C. The phase difference of the temperature change of adjacent crystals was 60°. The one period of the temperature change was 1000 seconds. Ambient gas was air and the pressure in the case was approximately 1.5×10^{-3} Pa.

The temperature of each crystal was measured with a thermistor sensor. The emitted X-rays were measured with a Si-PIN X-ray detector through a pinhole of 1.0 mm diameter formed in a lead sheet of 0.5 mm thickness. The effect of both the efficiency of the detector and the pinhole were corrected. Measurements were continuously repeated approximately 80 periods.



Figure 1. Photograph of the X-ray source.



(a) Top view.

(b) Side view.

Figure 2. Schematic of the X-ray source.

3. Results and Discussion

Figure 3 shows the time characteristics of the X-ray intensity per period which is integrated in the energy range from 2.5 keV to 40 keV. As Fig. 3 shows X-rays were continuously emitted. Moreover, it was found that the counting rate was dependent on the case material. In each case, the difference in the counting rate for each peak is due to the slight difference of the crystal position or the ΔT .

Table 1 shows the average counting rate and the ripple factor which are calculated from Fig. 3. The ripple factor is defined as the ratio of the root mean square (RMS) value of the ripple to the average value. The average counting rate of the stainless steel and the Al case is 3 and 4.8 times, respectively, as much as that of Cu case. Furthermore, there is the tendency that the ripple factor increases when the average counting rate increases. It is suggested that the amount of electrons supplied through the interaction between the case material of an X-ray source and emitted X-rays is different.

When X-rays are incident upon the inner wall of the case, fluorescence X-rays and electrons are emitted. The electrons are emitted by both the photoelectric effect and the Auger process. Photoelectrons are easily emitted by the photoelectric effect for material with the low work function. Either the emission of fluorescent X-rays or the Auger process occurs after incident X-rays eject the inner-shell electron as a photoelectron [3]. Both are competitive processes and the Auger process tends to occur if fluorescence yield is small. Thus, it is expected that the amount of Auger electrons emitted by the interaction increase for material with low fluorescence yield. The photoelectrons and Auger electrons emitted by the interaction are immediately accelerated toward the crystal, the target and the case by the electric field. As a result, X-rays are emitted by the impact of electrons against them.

Table 2 shows the work function and the *K*-shell fluorescence yield of the case material [3, 4]. Stainless steel (SUS304) is composed of 74 % iron, 18 % chromium and 8 % nickel. As Table 2 shows, the fluorescence yield of Cr, Fe and Ni is lower than that of Cu, and that of Al is the lowest. Moreover, the work function of Al is also lower than the others. Thus, the amount of emitted photoelectrons and Auger electrons is the maximum for the case of Al.

Figure 4 shows the energy spectra of X-rays per period. Characteristic X-rays, Nb $K\alpha$ and Nb $K\beta$ were observed and are originated from the target. The others are originated from crystals and the case material. The intensity of Nb $K\alpha$ and Nb $K\beta$ X-rays are higher than the others. Characteristic X-rays except Nb $K\alpha$ and Nb $K\beta$ are not detected for the case of Al because the sensitivity of the Si-PIN detector is much weak for characteristic X-rays of Al.

Table 1. The average counting rate, the RMS value of the ripple and the ripple factor which are calculated from Fig. 3.

Case material	Average counting rate [cps]	RMS value of the ripple [cps]	Ripple factor
Cu	2.2×10^2	1.2×10^2	0.52
Stainless steel	6.8×10^2	4.6×10^2	0.67
Al	1.1×10^3	7.8×10^2	0.73

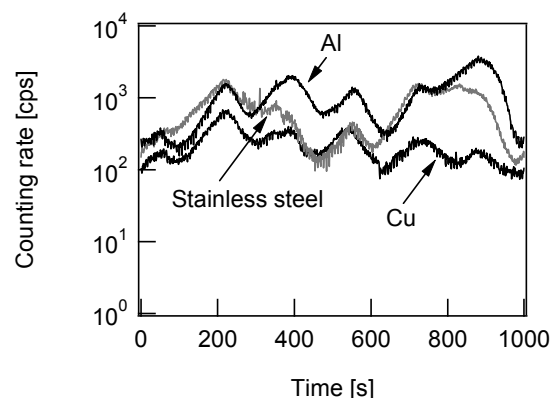


Figure 3. Time characteristics of the X-ray intensity per period which is integrated in the energy range from 2.5 keV to 40 keV.

Table 2. Values of work function and fluorescence yield for each case material.

Element	Work function ϕ [eV]	Fluorescence yield ω_K
Al	4.28	0.03872
Cr	4.5	0.2885
Fe	4.5	0.3546
Ni	5.15	0.4212
Cu	4.65	0.4538

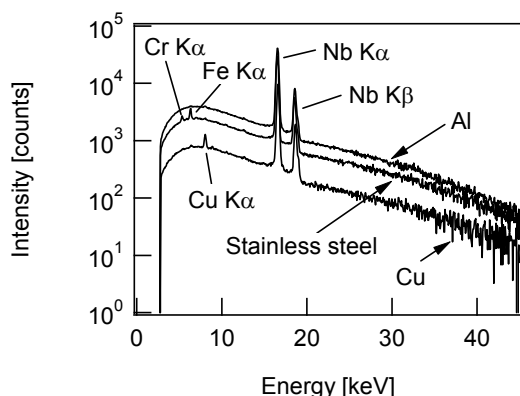


Figure 4. Energy spectra of X-rays per period.

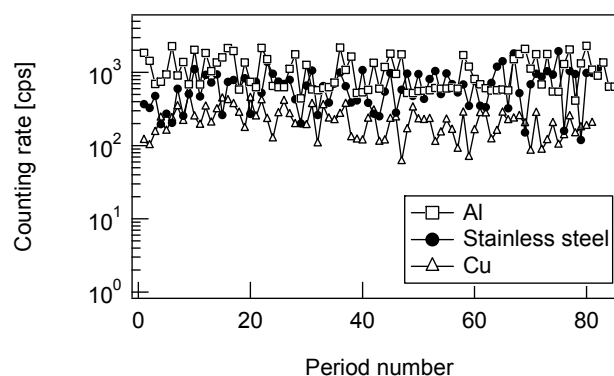


Figure 5. Cyclic characteristics of the average counting rate in each period.

Figure 5 shows the cyclic characteristics of the average counting rate in each period. Table 3 shows the coefficient of variation (*CV*) which is calculated from Fig. 5. The *CV* is defined as the ratio of the standard deviation to the average. The *CV* and the counting rate shown in Fig. 5 indicate that the average counting rate fluctuates through the periods. This might be due to the creeping discharge on the crystal surface which occurs irregularly. When a spike-like current flows into the crystal surface, the electric fields disappear suddenly because the discharge instantaneously neutralizes charges on the $-z$ surface. Thus, emission of X-rays stops irregularly and the average counting rate fluctuates through the periods.

As shown in Fig. 5, the average counting rate for the case of Cu decreased with increasing the temperature cycle. It is speculated that the main factor of this result is the decrease of the amount of the generated electrons. When X-rays are emitted for a long time, the amount of electrons consumed for X-ray emission and supplied electrons will reach the equilibrium state. Thus, it is expected that the average counting rate of each period will become constant when X-rays are emitted for a long time.

Table 3. The average counting rate, the standard deviation and the *CV* which are calculated from Fig. 5.

Case material	Average counting rate [cps]	Standard deviation [cps]	<i>CV</i>
Cu	2.2×10^2	9.9×10^1	0.44
Stainless steel	6.8×10^2	3.7×10^2	0.54
Al	1.1×10^3	5.6×10^2	0.52

4. Conclusion

In order to improve the intermittence of X-ray emission and the intensity, the X-ray source with the six LiTaO₃ single crystals was proposed. Furthermore, in order to investigate the emission of electrons by the interaction between the case material of an X-ray source and emitted X-rays, the three kinds of case material, oxygen-free copper, stainless steel and aluminum, with the different work function and the different fluorescence yield were used. The X-rays were emitted continuously. Moreover, the intensity of emitted X-rays was depended on the kind of case material and became high with decreasing the fluorescence yield of the case material. The intensity of the case of the Al was highest. It was suggested that a part of emitted electrons were by an Auger process.

References

- [1] Brownridge J D and Raboy S 1999 *J. Appl. Phys.* **86** 640
- [2] Guan Y, Fukao S, Ito K, Nakanishi Y, Sato Y, Ito Y and Yoshikado S 2010 *Key Eng. Mater.* **445** 43
- [3] Michaelson H B 1977 *J. Appl. Phys.* **48** 4729
- [4] Hubbell J H, Trehan P N, Singh N, Chand B, Mehta D, Garg M L, Garg R R, Singh S and Puri S 1994 *J. Phys. Chem. Ref. Data.* **23** 339